Continuous p-n junction with extremely low leakage current for micro-structured solid-state neutron detector applications

Kuan-Chih Huang*[a], Rajendra Dahal[a,b], James J.-Q. Lu[a], Yaron Danon[b], Ishwara B. Bhat[+a]
[a]Department of Electrical, Computer, and Systems Engineering, Rensselaer Polytechnic Institute, 110 Eighth Street, Troy, NY USA 12180; [b]Department of Mechanical, Aerospace, and Nuclear Engineering, Rensselaer Polytechnic Institute, 110 Eighth Street, Troy, NY USA 12180

ABSTRACT

Considerable progress has been achieved recently to enhance the thermal neutron detection efficiency of solid-state neutron detectors that incorporate neutron sensitive materials such as ^{10}B and ^{6}LiF in Si micro-structured p-n junction diode. Here, we describe the design, fabrication process optimization and characterization of an enriched boron filled honeycomb structured neutron detector with a continuous p^+-n junction. Boron deposition and diffusion processes were carried out using a low pressure chemical vapor deposition to study the effect of diffusion temperature on current density-voltage characteristics of p^+-n diodes. TSUPREM-4 was used to simulate the thickness and surface doping concentration of p^+-Si layers. MEDICI was used to simulate the depletion width and the capacitance of the micro-structured devices with continuous p^+-n junction. Finally, current density-voltage and pulse height distribution of fabricated devices with 2.5×2.5 mm^2 size were studied. A very low leakage current density of ~2×10^{-8} A/cm^2 at -1 V (for both planar and honeycomb structured devices) and a bias-independent thermal neutron detection efficiency of ~26% under zero bias voltage were achieved for an enriched boron filled honeycomb structured neutron detector with a continuous p^+-n junction.

Keywords: Thermal neutron detector, micro-structured detector, boron deposition, boron diffusion, low-pressure chemical vapor deposition, low leakage current, continuous p-n junction

*huangk6@rpi.edu
+bhati@rpi.edu

1. INTRODUCTION

Since neutrons are a very specific indicator of fissile materials, neutron detectors possessing high neutron detection efficiency, low gamma sensitivity and large detection area are needed for homeland security. The existing gas filled detectors offer very high efficiency (>70 %), low noise and very low gamma sensitivity[1]. However, gas filled detectors have many shortcomings, such as poor portability, high gas pressure (~9 atm), high bias voltage (1000-2000 V) and high cost due to the limited supply of ^{3}He. Solid-state neutron detection is one of the emerging technologies as an alternative to the ^{3}He gas filled detectors to solve the long-term shortage of ^{3}He gas. Most of the solid-state neutron detectors are fabricated by coating a thin layer of neutron sensitive material with large absorption cross-section (^{10}B or ^{6}LiF for example) on top of a Si or GaAs p-n diode[2,3,4]. When a neutron interacts with ^{10}B, energetic daughter particles, alpha particle and ^{7}Li ion, are generated. As daughter particles enter a p-n junction diode, electron-hole pairs (EHPs) are created due to the impact ionization. EHPs created inside the depletion region and within a diffusion length from the depletion region edge are separated by the built-in electric field and then collected as voltage signals by external electronic circuit. In this type of converter-layer-coated planar detector, neutron detection efficiency is limited to only 2-5% due to the conflicting requirement of converter layer thickness for large absorption length for incoming thermal neutrons (~45 μm for 90% interaction of neutrons in ^{10}B) as well as short escape length for daughter particles (2-3 μm for daughter particles in ^{10}B)[5]. The widely adopted approach to overcome the low neutron detection efficiency in planar devices is the use of micro-structured pillar or parallel stripe p-i-n diodes in which the gap between pillars or stripe is filled with either ^{6}LiF or ^{10}B[6,7]. These composite micro-structures are designed in such a way that converter material is thick enough for most of incident neutron absorption and at the same time thin enough to allow daughter particles to escape sideways. Although the overall neutron detection efficiency of the micro-structured neutron detector has been increased, the unpassivated etched Si wall leads to a high leakage current, which not only increases the device electronic noise but also limits the detection area of the device to only several square millimeters[6,7,8].

Chemical, Biological, Radiological, Nuclear, and Explosives (CBRNE) Sensing XIV, edited by Augustus Way Fountain, Proc. of SPIE Vol. 8710, 87101J · © 2013 SPIE · CCC code: 0277-786X/13/$18 · doi: 10.1117/12.2016121

Our group has proposed and demonstrated a boron filled Si honeycomb structured neutron detector with a continuous p^+-n junction[9]. The composite structure of boron and Si is a prime choice for fabricating thermal neutron detectors because Si has low ionization energy for EHP generation (~3.62 eV)[10], high crystal quality and low gamma sensitivity to serve as an excellent host semiconductor along with low cost and matured device processing technology. Besides, boron is an excellent converter material due to its high thermal neutron absorption cross-section of ~3837 barns and high compatibility with Si processing technology. GEANT4 Monte Carlo simulation of honeycomb/hexagonal hole geometry with enriched boron filling shows that the thermal neutron detection efficiency up to 48% (for 2.8 μm wide by 45 μm deep holes separated with 1 μm thick Si wall) is possible for thermal neutron flux incident normal to the detecting surface[11]. Even higher intrinsic thermal neutron detection efficiency is expected for isotropic neutron flux because of an increased effective absorption length[12]. Like other microstructures, controlling leakage current due to surface recombination in etched surface of hexagonal holes is a difficult task. We have employed a novel concept of forming a continuous p^+-n junction over the entire Si surface of honeycomb structured neutron detectors by using the initial portion of boron filling process followed by boron diffusion process in low pressure chemical vapor deposition (LPCVD)[13,14]. Continuous p^+-n junction not only reduces the reverse leakage current due to the etched Si wall but also fully depletes the Si wall with optimized Si wall thickness and p^+-Si and n-Si doping concentration in order to maximize the charge collection and reduce the device capacitance under no external bias. This type of detector can be operated in photovoltaic mode without losing efficiency and the photovoltaic mode of operation also helps to limit leakage current in large-area detectors. Therefore, the maximum possible device size of such micro-structured detector depends on both capacitance and leakage current. Although the formation of the continuous p^+-n junction offers a significant improvement, the effect of boron diffusion process as a part of boron filling process on the detector performance, such as leakage current, device capacitance and neutron detection efficiency, needs to be further discussed.

In this work, we summarize the design, fabrication process optimization and finally characterization of enriched boron filled honeycomb structured neutron detector with a continuous p^+-n junction. The fabrication process optimization also includes the boron diffusion temperature optimization in LPCVD. The current density-voltage (J-V) characteristics for p^+-n diodes fabricated with different diffusion temperature were studied. Taurus TESUPREM-4 and MEDICI programs were used to simulate the boron diffusion process of p^+-n diodes and the depletion width and device capacitance of micro-structured devices with continuous p^+-n junction, respectively. Finally, a boron filled honeycomb structured neutron detector with a continuous p^+-n junction was fabricated on a Si epitaxial wafer using optimized boron diffusion temperature. A planar neutron detector was also fabricated on the same Si epitaxial wafer for reverse leakage current comparison. Reverse leakage current and neutron detection efficiency of such honeycomb structured neutron detector were measured in order to elucidate the significance of the continuous p^+-n junction.

2. EXPERIMENTAL METHOD

2.1 Sample preparation

In the first part of the present work, we conducted the boron diffusion process optimization in LPCVD to fabricate a high quality p-n junction diode. For this purpose, a 4-inch lightly doped (100) oriented n-Si wafer (resistivity ~12 Ω-cm) was used as a starting substrate. Ion implantation was performed to fabricate an n^+-Si layer (surface doping concentration ~10^{19} cm^{-3}) on the backside for ohmic contact formation. An ~1.5 μm thick silicon dioxide (SiO_2) layer was deposited on the front side and then etched off from the device area using wet buffered oxide etch (BOE) to define each device dimension as 2.5×2.5 mm^2. The wafer was then diced into four pieces as starting wafers. Three starting wafers were used to investigate the boron diffusion process conducted at diffusion temperature of 700, 800 and 900 °C, respectively (Fig.1 (a)). One starting wafer was used to fabricate Schottky diodes by directly depositing Al with 2% Si on the front side and Ti/Al on the backside of the starting wafer for metal contacts. The planar neutron detector (Fig.1 (b)) and honeycomb structured neutron detector (Fig.1 (c)) were fabricated on a 4-inch moderately doped (100) n-Si wafer (resistivity ~0.5 Ω-cm) with an ~50 μm thick lightly doped n-Si epitaxial layer (~50 Ω-cm) and an ~1 μm thick heavily doped p^+ Si epitaxial layer (~0.01 Ω-cm). The details of honeycomb structured neutron detector fabrication are given in our earlier publications[13,14].

2.2 Boron deposition and diffusion process

LPCVD was used to deposit enriched boron (99.9% ^{10}B) films on the three n-Si bulk wafers with a precursor gas of diluted enriched diborane (1% B_2H_6 in H_2). During the deposition process, wafers were placed on a graphite susceptor that was inductively heated to ~510 °C in a water-cooled horizontal quartz reactor for 5 minutes. After the deposition,

boron diffusion was carried out in succession in the same reactor for 10 minutes at 700, 800 and 900 °C each to form p^+ Si layers.

2.3 Boron wet etching process

After the diffusion process, remaining boron films on the three n-Si bulk wafers were removed by immersing the wafers in a 50 °C hydrogen peroxide (H_2O_2) and ethanol (C_2H_6O) mixture (One part of H_2O_2 in five part of C_2H_6O by volume). Etch rate of boron is ~400 nm/hour. In this etching process, H_2O_2 was used to oxidize boron to form boron oxide, which is soluble in C_2H_6O. Finally, an ~1.5 µm thick Al with 2% Si was sputtered on the front side and an ~100 nm thick titanium followed by an ~900 nm thick Al were sputtered on the backside for ohmic contacts. Front-side metal was removed from the grid area using photolithography and a standard Al wet etching technique to isolate each device.

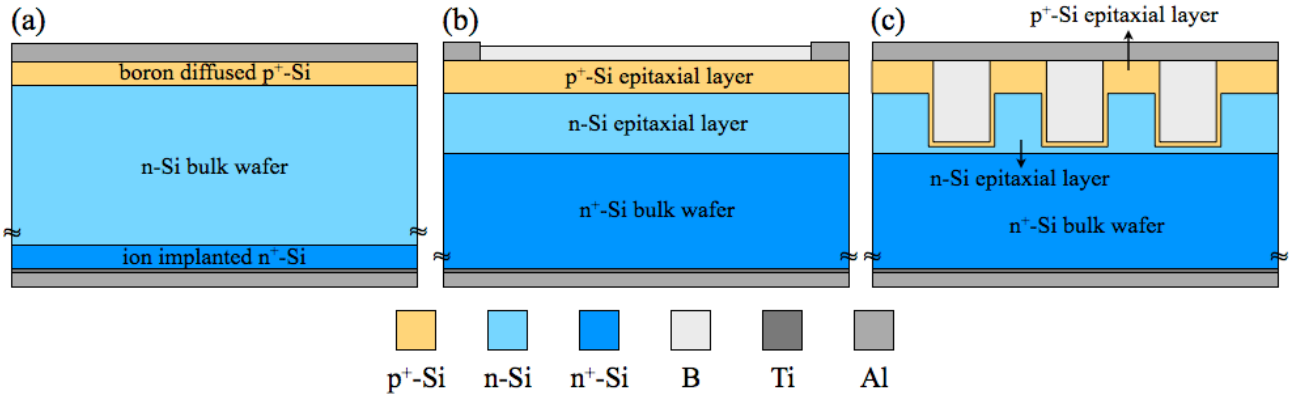

Figure 1. Schematics for (a) p^+-n diode fabricated using Si bulk wafer, (b) planar neutron detector and (c) honeycomb structured neutron detector with a continuous p^+-n junction fabricated using Si epitaxial wafer.

3. RESULTS AND DISCUSSION

3.1 Current-voltage characteristics for p^+-n diodes

Figure 2(a) shows forward and reverse J-V characteristics of a Schottky diode and three p^+-n diodes with boron diffusion performed at 700, 800 and 900 °C, respectively. Diffusion at 800 and 900 °C show lower reverse leakage current density on the order of 10^{-6} A/cm^2 at -1 V. However, diffusion at 700 °C shows higher reverse leakage current density on the order of 10^{-4} A/cm^2 at -1 V, which is close to the reverse leakage current of the Schottky diode. It is possible that both Schottky diode and p^+-n diode behavior is observed since the p^+-Si layer may be very thin and not fully continuous over the entire surface. Figure 2(b) shows only the forward I-V characteristics of the Schottky diode and the three p^+-n diodes with the ideality factor labeled in different regions and series resistance labeled at high current level. The ideality factor (n) is derived from the slope of Ln(I)-V curves based on the diode equation $I = I_0(e^{\frac{qV}{nkT}} - 1)$. Series resistance ($r_s$) is calculated from the deviation of the I-V curve from linearity at high current level according to $\Delta V = Ir_s$. If all three diffusion processes resulted in p^+-Si layers, the forward and reverse J-V characteristics of all three p^+-n diodes should be similar since lightly doped n-Si region of the bulk wafer mainly determines the current. Besides, the series resistance of the p^+-n diodes should be significantly lower than that of the Schottky diode due to conductivity modulation in high forward bias. P^+-n diodes with boron diffusion performed at 800 and 900 °C show a reasonably good diode behavior based on the ideality factor and their substantially low reverse leakage current compared to the p^+-n diode with boron diffusion performed at 700 °C. The higher ideality factor of the p^+-n diode with boron diffusion performed at 900 °C at low current level is possibly because of the shunt resistance of the diode. The series resistance of the p^+-n diodes with boron diffusion performed at 800 and 900 °C are ~10.3 Ω and ~10.7 Ω, which are very close to that of the n-Si bulk wafer due to low series resistance of the p^+-Si layers and good metal contacts. As the p^+-Si layer of the p^+-n diode with boron diffusion performed at 700 °C may be very thin and even not continuous, the series resistance is relatively high (~23.3 Ω). This may be resulted from the contribution of both p^+-n diode and Schottky diode (~144.4 Ω).

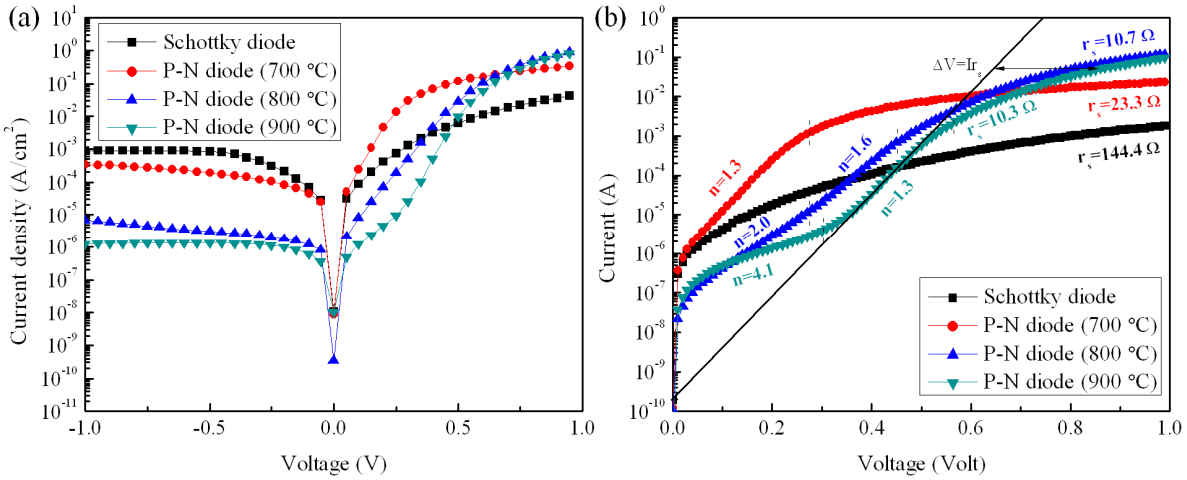

Figure 2. (a) Forward and reverse J-V characteristics of a Schottky diode and three p^+-n diodes with boron diffusion performed at 700, 800 and 900 °C and (b) forward I-V characteristics of the Schottky diode and the three p^+-n diodes with the ideality factor labeled in different regions and series resistance labeled at high current level.

3.2 TSUPREM-4 simulation for boron diffusion process

Figure 3 shows TSUPREM-4 simulations of boron diffusion process conducted at diffusion temperature of 700, 800 and 900 °C, respectively[15]. Red, blue and green curves indicate the boron diffusion profiles conducted at 700, 800 and 900 °C respectively and black curve shows the background doping concentration. Diffusion at 700, 800 and 900 °C result in ~5, ~25 and ~110 nm thick p^+-Si layer with the surface doping concentration of ~1.2×10^{19}, ~4.5×10^{19} and ~1.1×10^{20} 1/cm^3, which are very close to the solid solubility of boron in Si resulted from the infinite boron source on the Si surface[16]. In our honeycomb structured neutron detector, because only the EHPs created by daughter particles inside the depletion region and a diffusion length away from the depletion region edge are able to be collected by anode and cathode contacts, neutral p^+-Si region needs to be thin enough to enable the creation of most EHPs inside the depletion region. Therefore, p^+-n diode having very thin p^+-Si layer and at the same time exhibiting good diode behavior is desired. Based on the results of J-V characteristics and TSUPREM-4 simulations, diffusion temperature of 800 °C was decided to be used in the diffusion process for forming a continuous p^+-n junction over the entire surface of honeycomb structured neutron detectors.

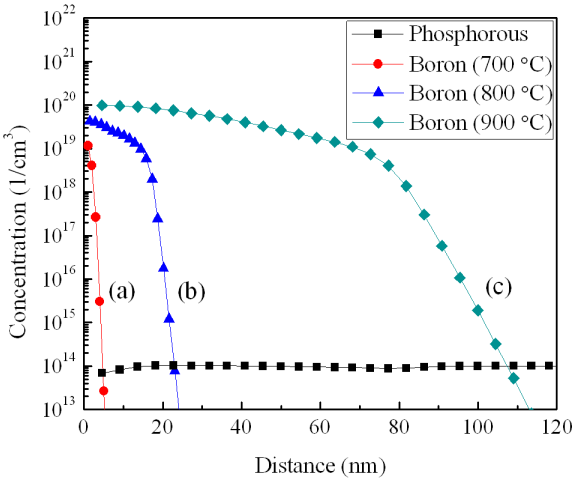

Figure 3. Taurus TSUPREM-4 simulations of boron diffusion process conducted at diffusion temperature of (a) 700 °C, (b) 800 °C and (c) 900 °C, respectively.

3.3 MEDICI simulation for depletion region and device capacitance

A continuous p^+-n junction with selected Si wall thickness as well as doping concentration of p^+-Si layer and n-Si substrate can fully deplete the Si wall. With fully depleted Si wall, the EHPs generated inside the depletion region and one diffusion length away from the depletion region edge are separated efficiently by the built-in electric field, which gives rise to a maximum charge collection under zero bias voltage. Besides, fully depleted Si wall reduces the device capacitance, which results in large electric signals based on the equation $V = \frac{Q}{C}$. In order to achieve the highest neutron detection efficiency, hexagonal hole diameter and Si wall thickness have to be kept at 2.8 μm and 1 μm respectively according to our simulation results[11]. Based on the optimized hole diameter and the properties of p^+-Si layer fabricated using diffusion temperature of 800 °C, MEDICI simulation was performed on a 1 μm wide by 45 μm tall trench structured n-Si substrate with a continuous p^+-Si layer over the entire surface as shown in Fig 4(a)[17]. Green, yellow and blue regions indicate n-Si with doping concentration of 1×10^{14} 1/cm^3, p^+-Si with doping concentration of 4.5×10^{19} 1/cm^3 and boron, respectively. Red dashed line indicates the depletion region edge. The Si wall for this case is fully depleted and the base depletion region depth is ~3 μm (~7 μm when n-Si doping concentration is 1×10^{13} 1/cm^3). Another MEDICI simulation was also performed to investigate the device capacitance as a function of n-Si substrate with different doping concentration used. Figure 4(b) shows the capacitance as a function of n-Si doping concentration with p^+-Si doping concentration and Si wall thickness kept at 4.5×10^{19} 1/cm^3 and 1 μm, respectively. The capacitance decreases when the n-Si doping concentration is deceased and the Si wall is only fully depleted when the n-Si doping concentration is below 1×10^{15} 1/cm^3. Since the range of daughter particles in Si is 2-5 μm, the portion of the base depletion region depth over this range will not contribute to the neutron detection efficiency but only interact with gamma rays, which leads to a high gamma sensitivity. Therefore, n-Si doping concentration of 1×10^{14} 1/cm^3 is selected to fully deplete our honeycomb structured neutron detector for obtaining maximum charge collection and large electric signal under zero bias, while maintaining low gamma sensitivity.

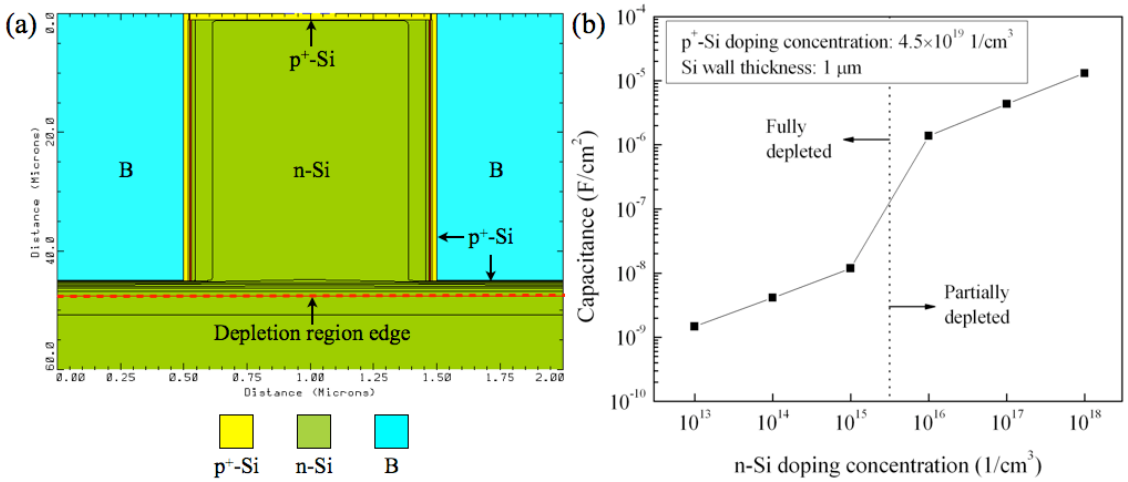

Figure 4. MEDICI simulation of (a) boron diffusion on a 1 μm wide by 45 μm tall trench structured n-Si substrate (1×10^{14} 1/cm^3) with a continuous p^+-Si layer (4.5×10^{19} 1/cm^3) over the entire surface and (b) capacitance as a function of n-Si doping concentration with p^+-Si doping concentration and Si wall thickness kept at 4.5×10^{19} 1/cm^3 and 1 μm.

3.4 Current-voltage characteristics for planar and honeycomb structured neutron detectors

Formation of continuous p^+-n junction over the micro-structured neutron detector is also designed to minimize the surface recombination from the etched Si wall for reducing reverse leakage current. To verify this, a 2.5×2.5 mm^2 planar neutron detector and a 2.5×2.5 mm^2 enriched boron filled honeycomb structured neutron detector with a continuous p^+-n junction were fabricated using a Si epitaxial wafer as shown in Fig 1(b) and 1(c). Figure 5 shows the I-V characteristics of the planar and the honeycomb structured detector with a continuous p^+-n junction. The reverse leakage current density of the planar detector is ~2.1×10^{-8} A/cm^2 and that of the honeycomb structured neutron detector is ~1.8×10^{-8} A/cm^2 at -1 V. Probably because silicon epitaxy growth process provides more high-quality silicon, the reverse leakage currents for the planar and the honeycomb structured neutron detectors as shown in Fig. 5 are lower than that for the p^+-n diodes fabricated in Si bulk wafer as shown in Fig. 2(a) due to longer minority carrier lifetime in n-Si epitaxial layer[18]. The very

low reverse leakage current density of our honeycomb structured neutron detector is the lowest for similar micro-structured solid-state neutron detector[6,7]. Since the reverse leakage current densities of the planar and honeycomb structured detectors are very close, the formation of the continuous p^+-n junction in LPCVD as a part of the boron filling process is proven to be effective to reduce the reverse leakage current and thus plays one of the pivotal roles in the fabrication of high-quality micro-structured p-n diodes. Our result of such a very low reverse leakage current density is significantly helpful for the fabrication of scalable large area neutron detectors.

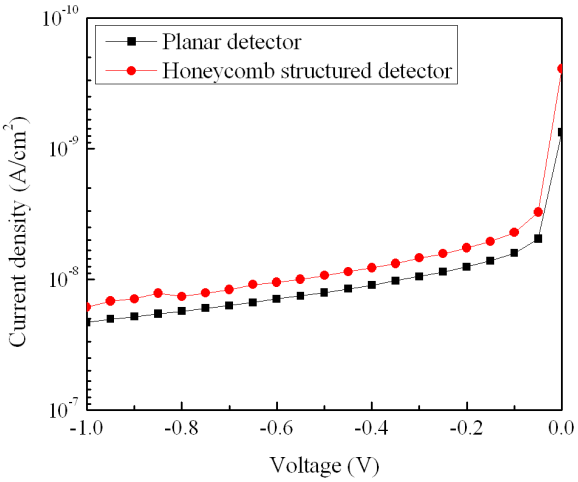

Figure 5. J-V characteristics of 2.5×2.5 mm^2 planar neutron detector and honeycomb structured neutron detector with a continuous p^+-n junction.

3.5 Neutron detection efficiency measurement

In order to verify that the Si wall in the detector is fully depleted experimentally, the thermal neutron detection efficiency of the honeycomb structured neutron detector was measured under different reverse bias voltages. Figure 6(a) shows a measured pulse height distribution of a 2.5×2.5 mm^2 enriched boron filled honeycomb structured neutron detector under zero bias voltage with x-axis normalized by assuming the spectrum endpoint is the full charge particle energy deposition (~2.5 MeV) based on GEANT calculation[19]. Figure 6(b) shows the neutron detection efficiency under reverse bias voltage of 0, 1 and 2 V. An uncollimated neutron beam is created by placing a californium-252 (^{252}Cf) source in a high-density polyethylene moderator housing. The detector was positioned at a distance of 10 cm where the average thermal neutron flux was ~798 neutrons/sec/cm^2 (black curve)[12]. In order to differentiate the counts registered by thermal neutrons, the moderator housing was covered with a 2 mm thick Cd shield to block thermal neutrons and allow fast neutrons and gamma rays to pass (red curve). In order to measure gamma sensitivity, the detector was positioned 4 cm away from a cobalt-60 (^{60}Co) source for obtaining 10 mR/h dose (blue curve). Finally, the total electronic noise resulted from the device leakage current as well as electronic system was measured with both ^{252}Cf and ^{60}Co sources removed from the room (green curve). It is clearly observed that the electronic noise level is below 70 keV, which is attributed to the extremely low leakage current due to the formation of continuous p^+-n junction over the entire surface of the detector. Although the electronic noise level is very low, the neutron detector also responds to gamma rays, which are registered below 400 keV. In order to avoid any contribution from gamma rays to the intrinsic neutron detection efficiency, the low level discriminator (LLD) was set at 400 keV. The Maxwellian averaged thermal neutron detection efficiency without bias is 26.1 ± 0.3% and the gamma sensitivity is ~10^{-5}. Same thermal neutron detection efficiencies were measured under the bias voltage of 1 and 2 V, which ensures that the Si wall has been fully depleted by the continuous p^+-n junction under zero bias.

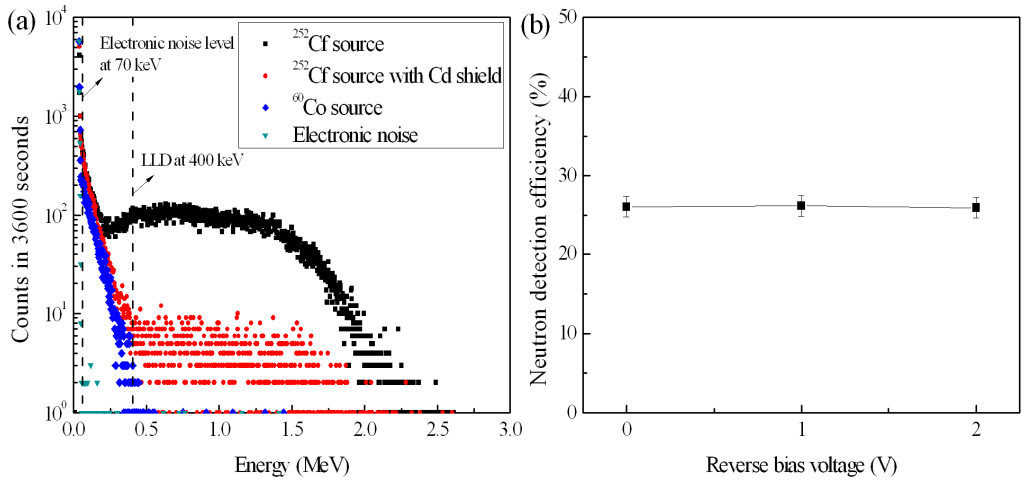

Figure 6. (a) Measured pulse height distribution of a 2.5×2.5 mm^2 enriched boron (99.9% ^{10}B) filled honeycomb structured neutron detector under zero bias voltage. The counts were recorded for 3600 seconds and the LLD is set at 400 keV and (b) neutron detection efficiency under reverse bias voltage of 0, 1 and 2 V.

4. CONCLUSIONS

In summary, J-V characteristics of p^+-n diodes fabricated by depositing and diffusing boron at different diffusion temperatures (700, 800, and 900 °C) as a part of boron filling process using LPCVD were studied. J-V characteristics show that diffusion at 800 and 900 °C result in reasonably good diode behavior and lower reverse leakage current compared to diffusion at 700 °C. The measured J-V characteristics and TSUPREM-4 simulations suggested that 800 °C is the best diffusion temperature due to high enough surface doping concentration and proper thickness of p^+-layer for charge collection. MEDICI simulations also confirm that Si wall in the honeycomb structured neutron detector is fully depleted by using the diffusion temperature of 700, 800 and 900 °C, which reduces the device capacitance that helps to get large signal to noise ratio. A 2.5×2.5 mm^2 enriched boron filled honeycomb structured neutron detector with a continuous p^+-n junction formed by using the initial portion of boron filling process shows the leakage current density of ~2×10^{-8} A/cm^2 at -1 V, which is comparable to that of a planar detector. Furthermore, thermal neutron detection efficiency of ~26% was achieved for a single layer detector and the efficiency is found to be independent of applied reverse bias voltage indicating that Si wall is fully depleted under zero bias. These results are very promising for the emerging field of solid-state neutron detector applications.

ACKNOWLEDGEMENT

The authors would like to thank the support and input of the support staff of the Rensselaer Polytechnic Institute Micro-Nano-Clean-Room (RPI MNCR) and Cornell NanoScale Science & Technology Facility (CNF). This work is supported by DOE—Nuclear Energy University Programs (NEUP), Award No. DE-AC07- 05ID14517.

REFERENCES

[1] Veloso J. F. C. A., Amaro F., dos Santos J. M. F., Mir J. A., Derbyshire G. E., Stephenson R., Rhodes N. J., and Schooneveld E. M., "Application of the microhole and strip plate detector for neutron detection," IEEE Trans. Nucl. Sci. 51, 2104 (2004).
[2] Rose A., "Sputtered boron films on silicon surface barrier detectors," Nucl. Instrum. Methods 52, 166 (1967).
[3] Petrillo C., Sacchetti F., Toker O., and Rhodes N. J., "Solid state neutron detectors," Nucl. Instrum. Methods Phys. Res. A 378, 541 (1996).

[4] McGregor D. S., Hammig M. D., Yang Y.-H., Gersch H. K., and Klann R. T., "Design considerations for thin film coated semiconductor thermal neutron detectors—I: basics regarding alpha particle emitting neutron reactive films," Nucl. Instrum. Methods Phys. Res. A 500, 275 (2002).
[5] McGregor D. S., Klann R. T., Gersch H. K., and Yang Y.-H., "Thin-film-coated bulk GaAs detectors for thermal and fast neutron measurements," Nucl. Instrum. Methods Phys. Res. A 466, 126 (2001).
[6] Nikolic R. J., Conway A. M., Reinhardt C. E., Graff R. T., Wang T. F., Deo N., and Cheung C. L., "6 : 1 aspect ratio silicon pillar based thermal neutron detector filled with (10)B," Appl. Phys. Lett. 93, 133502 (2008).
[7] McGregor D. S., McNeil W. J., Bellinger S. L., Unruh T. C., and Shultis J. K., "Microstructured semiconductor neutron detectors," Nucl. Instrum. Methods Phys. Res. A 608, 125–131 (2009).
[8] Yoon H. P., Yuwen Y. A., Kendrick C. E., Barber G. D., Podraza N. J., Redwing J. M., Mallouk T. E., Wronski C. R., and Mayer T. S., "Enhanced converter efficiencies for pillar array solar cells fabricated from crystalline silicon with short minority carrier diffusion lengths," Appl. Phys. Lett. 96, 213503 (2010).
[9] LiCausi N., Dingley J., Danon Y., Lu J.-Q., and Bhat I. B., "A novel solid-state self-powered neutron detector," Proc. SPIE 7079, 707908 (2008).
[10] Pehl R. P., Goulding F. S., Landis D. A., and Lenzlinger M., "Accurate determination of the ionization energy in semiconductor detectors," Nucl. Instrum. Methods 59, 45–55 (1968).
[11] Dingley J., Danon Y., LiCausi N., Lu J.-Q., and Bhat I. B., "Optimization of a novel solid-state self powered neutron detector," 2009 International Conference on Mathematics, Computational Methods & Reactor Physics, Saratoga Springs, NY.
[12] Dingley J., Danon Y., LiCausi N., Lu J.-Q., and Bhat I. B., "Directional Response of Microstructure Solid State Thermal Neutron Detectors," Trans. of the American Nuclear Society and Embedded Topical Meeting Isotopes for Medicine and Industry 103, 214–215 (2010).
[13] Dahal R., Huang K.-C., Clinton J., Licausi N., Lu J.-Q., Danon Y., and Bhat I. B., "Self-powered micro-structured solid state neutron detector with very low leakage current and high efficiency," Apply. Phys. Lett. 100, 243507 (2012).
[14] Huang K.-C., Dahal R., Lu J.-Q., Danon Y., and Bhat I. B., "Boron filling of high aspect ratio holes by chemical vapor deposition for solid-state neutron detector applications," J. Vac. Sci. Technol. B 30, 051204 (2012).
[15] Synopsys, "Taurus TSUPREM-4, User Guide, Version Z-2007.3," Synopsis Inc., Mountain View, CA (2007).
[16] Vick G. L. and Whittle K. M., "Solid solubility and diffusion coefficients of boron in silicon," J. Electrochem. Soc. 116, 1142–1144 (1969).
[17] Synopsys, "Taurus MEDICI, User Guide, Version D-2010.3," Synopsis Inc., Mountain View, CA (2010).
[18] Ciszek T. F., Wang T., Schuyler T., and Rohatgi A., "Some effects of crystal growth parameters on minority carrier lifetime in floated-zoned silicon," J. Electrochem. 136, 230–234 (1989).
[19] Agostinelli S., Allison J., Amako K., Apostolakis J., Araujo H., Arce P., Asai M., Axen D., Banerjee S., and Barrand G., "GEANT4 - A Simulation Toolkit," Nucl. Instrum. Methods Phys. Res., Sect. A 506, 250 (2003).